JACS
JOURNAL OF THE AMERICAN CHEMICAL SOCIETY
Communication
pubs.acs.org/JACS

High-Throughput Examination of Fluorescence Resonance Energy Transfer-Detected Metal-Ion Response in Mammalian Cells

Hairong Ma,[†,‡] Emily A. Gibson,[†,§] Philip J. Dittmer,[†] Ralph Jimenez,*[,†,‡] and Amy E. Palmer*[,†]

[†]Department of Chemistry and Biochemistry, University of Colorado, Boulder, Colorado 80309, United States
[‡]JILA, University of Colorado Boulder and NIST, Boulder, Colorado 80309, United States

Supporting Information

ABSTRACT: Fluorescence resonance energy transfer (FRET)-based genetically encoded metal-ion sensors are important tools for studying metal-ion dynamics in live cells. We present a time-resolved microfluidic flow cytometer capable of characterizing the FRET-based dynamic response of metal-ion sensors in mammalian cells at a throughput of 15 cells/s with a time window encompassing a few milliseconds to a few seconds after mixing of cells with exogenous ligands. We have used the instrument to examine the cellular heterogeneity of Zn^{2+} and Ca^{2+} sensor FRET response amplitudes and demonstrated that the cluster maps of the Zn^{2+} sensor FRET changes resolve multiple subpopulations. We have also measured the in vivo sensor response kinetics induced by changes in Zn^{2+} and Ca^{2+} concentrations. We observed an ~30 fold difference between the extracellular and intracellular sensors.

Genetically encoded fluorescent biosensors have revolutionized the study of dynamic processes in live cells and provided important information about the mechanisms of a vast array of cellular processes ranging from Ca^{2+} homeostasis to kinase activity.[1−3] Over 120 sensors that exhibit fluorescence responses to diverse analytes are now available.[3] These fluorescence resonance energy transfer (FRET)-based sensors have the potential to create time-dependent concentration or activity maps of ions, small ligands, or macromolecules in living cells. To meet the challenge of multidimensional visualization, the dynamic range and response kinetics of the biosensors are critical attributes, since they directly affect the sensor's spatial and temporal resolution. Furthermore, biological measurements are inherently heterogeneous, with different levels of cell-to-cell variation.[4] The observed variability may arise from heterogeneity of the sensor molecules reporting the measurement or from intrinsic biological variability. Characterizing the population-based heterogeneity is important: for the former, it determines the sensor's sensitivity and resolving power, and for the latter, resolving the cell-to-cell variability is a critical step toward understanding the origin and mechanisms of biological noise.

A method capable of defining these properties with high-throughput and single-cell resolution is essential for characterizing sensors in cell populations or cell-based libraries and streamlining further refinement of the fluorescent sensor toolbox. Available bioanalytical methods are limited in their ability to perform this task. Fluorescence-activated cell sorting (FACS)[5] is a powerful high-throughput method for screening or sorting cells on the basis of their fluorescence properties. However, the measured signals reflect single snapshots of cellular states and thus provide little information about the dynamics or kinetics of a particular process. Automated fluorescence microscopy of single bacterial cells has been carried out in microfluidics arrays to study the gene-expression dynamics of a library with 1400 strains,[6] yet this approach involving one library member per microfluidic channel makes it difficult to extend the application to larger libraries or cell populations. Other methods such as stopped-flow spectroscopy[7] can be used to measure the in vitro kinetics of a chemical reaction with submillisecond time resolution but generally cannot be employed for measurements on living mammalian cells (with the exception of one hematopoietic murine cell line that can survive turbulent mixing in a stopped-flow mixer with 10 ms time resolution[8]) or for single-cell manipulation (stopped-flow methods provide a population average) and hence are not suited for cell-based assays in a high-throughput fashion.

Here we describe a time-resolved microfluidic flow cytometer [Figure 1a,b and Figure S1 in the Supporting Information (SI)] that can be used to examine FRET changes, heterogeneity, and kinetics of biochemical reactions at the single-cell level. Cellular reactions are initiated in individual cells using controlled fluid flow in microfluidics,[9−11] and the reaction progress is probed with FRET sensors. Micron-scale laminar flow[12] and hydrodynamic focus techniques[13] enable us to achieve rapid reaction initiation, accurate flow control, and high-throughput detection at the single-cell level. A flow-control valve system (Figure 1c) isolates the cell and buffer reservoirs and provides uninterrupted buffer switching. Pressure-driven streams of cells and buffers flow into the microfluidics device and meet at the entry junction (Figure 1d). At the junction, the cells are rapidly exposed to chemicals carried in the buffer streamline, hydrodynamically focused to a single file, and subjected to fluorescence interrogation as they pass through the two laser beams, which are separated by a delay line whose length varies. The detected signal is a train of Gaussian pulses, with the pulse width determined by the cell dwell time in the excitation beam. To pair-match the pulses from the same cell in this signal train (Figure 2a), the flow speed along the channel is adjusted using a double hydrodynamic focusing method (Figure 1d) so that

Received: November 7, 2011
Published: January 19, 2012

   dx.doi.org/10.1021/ja2101592 | J. Am. Chem.Soc. 2012, 134, 2488−2491

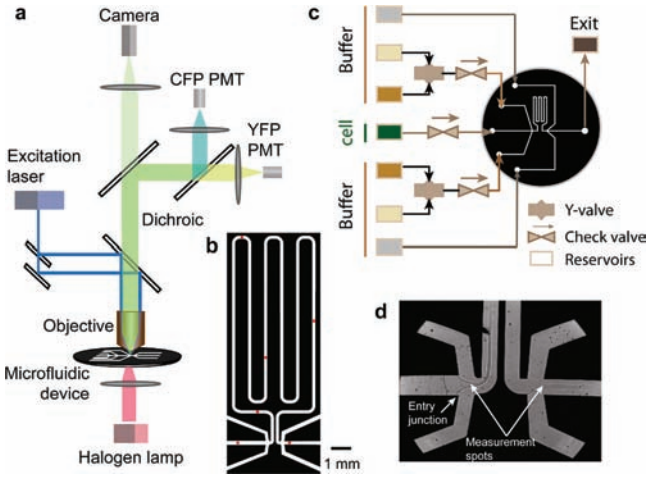

Figure 1. Experimental setup of the high-throughput microfluidics platform for dynamic FRET measurement in living cells. (a) Excitation/detection scheme for measurment of FRET in microfluidics. (b) Representative channel design of a microfluidics device (delay line length ~60 mm). A number of cells (depicted as red dots, size not to scale) may flow inside the interrogation channel concurrently. (c) Flow-control valve system. (d) Image of on-device microfluidics flow. The arrows show the positions of the cell buffer entry junction and the fluorescence measurement spots.

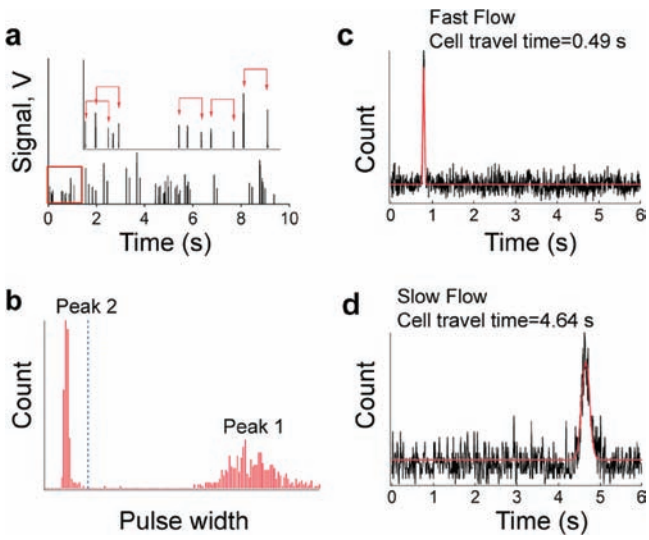

Figure 2. Data analysis and pair-matching algorithm. (a) Signal train generated by fluorescent cells traversing through the excitation laser beams. (b) Distribution of pulse widths (standard deviation of Gaussian fitting) at the two measurement spots; the different widths are due to the different flow speeds generated by the double hydrodynamic focusing method. (c, d) The interpulse interval histogram is extracted from the pulse train by assuming a trial n_{crowd} and counting the time intervals falling in different time bins. The cell travel time is obtained from the histogram. (c) Short travel time at high pressure. (d) Long travel time at low pressure.

the pulse widths are different at the two measurement spots. Using this method, which "labels" the signals at different measurement spots (Figure 2b), we are able to extract the cell travel time (Figure 2c,d) and match signal pairs within the signal train when a number of cells (n_{crowd}) are flowing inside the interrogation channel concurrently (Figures 1b and 2a). The pair-matching efficiency is >85% in the worst-case scenario (n_{crowd} > 5) (Figure S2). The measurements reported here were carried out in devices with a delay line length of ~60 mm, except for the D3pD surface display sensors, for which shorter delay lines of 4 or 8 mm were also used to produce time intervals down to 1 ms. With precise flow control and flexible device design, the cell travel time can be tuned within a time window between 1 ms and 10 s while maintaining the throughput of time-resolved single-cell FRET evaluation. Under our typical experimental conditions (described in the SI), the system is capable of measuring one-spot FRET at a throughput of >50 cells/s or FRET changes for individual cells at a throughput up to 15 cells/s.

We demonstrated the utility of this method for two applications: quantitative screening of cell-to-cell heterogeneity and measurement of millisecond time-resolved in vivo kinetics. For the first application, this method permits initiation of cellular reactions in a few milliseconds, measurement of FRET ratio changes with single-cell resolution, and analysis of FRET variability at the population level. For the second application, our instrument permits precise microfluidic flow control to measure the response kinetics of the sensors in their native cellular environment within time windows from 1 ms to 10 s. This time span is an important physiologically relevant domain in which numerous biological reactions (e.g., protein folding and synaptic vesicle endocytosis[14,15]) occur. However, it is a particularly difficult time window for kinetics measurements of cellular processes using fluorescence microscopy because the relatively slow macroscopic diffusion and mixing often occur on comparable time scales and hence could significantly interfere with the measured dynamics. Here we employ microfluidics techniques to reduce the diffusion-controlled mixing time to a few milliseconds.

The diffusion time obeys a square relationship with distance. Hence, with hydrodynamic focusing techniques[13] in which the cell-containing stream is squeezed to a 10 μm "jet" by the two analyte-containing buffer solutions, the time for the molecules to reach the cells can be significantly reduced. Figure S3 shows the simulated Ca^{2+} concentration field as a 2D surface image and 1D cross-section plots. The concentration profile along the cross section demonstrates that Ca^{2+} rapidly penetrates the center of the hydrodynamic focus, reaching ~3 mM at ~2.5 ms after the entry junction. This concentration is ~1000-fold higher than the minimum saturation point of the metal sensors, which have dissociation constants in the pico- to micromolar range.

We measured the FRET response kinetics and response heterogeneity of HeLa cells expressing intracellular Ca^{2+} and Zn^{2+} sensors. In particular, we employed genetically encoded Ca^{2+} sensors (D3cpV[16] expressed in the cytosol and D3pd displayed on the extracellular surface) and one Zn^{2+} sensor (ZapCY1[17] expressed in the cytosol). These sensors report concentration changes of intra- or extracellular metal ions by recruiting one or a few metal ions to their metal-binding domains, inducing a conformational change leading to a higher efficiency of FRET between the donor, cyan fluorescent protein (CFP), and the acceptor, yellow fluorescent protein (YFP) (Figure S4).

We first confirmed that metal-binding reactions could be induced in microfluidics flow and observed as FRET changes. Prior to the microfluidics experiment, cells were pretreated with metal chelators (e.g., EGTA for Ca^{2+} or TPEN for Zn^{2+}) to deplete the sensors of the targeted metal ions, thus maintaining the sensors in a metal-free state with a minimum FRET ratio. In control experiments, the cells showed no change in their

dx.doi.org/10.1021/ja2101592 | J. Am. Chem.Soc. 2012, 134, 2488–2491

ratiometric FRET values when mixed with metal-free buffer streams containing chelators (Figure S5). In addition, fluorescent beads (unresponsive to metal-ion perturbation) were doped into the D3cpV cell population to serve as an internal calibration of the reaction. In the response measurement, buffer streams contained metal ions, resulting in cell exposure within milliseconds of the entry junction. As expected from the sensor design, the cells showed a significant FRET increase after a time delay of >1 s (Figure 3a,c).

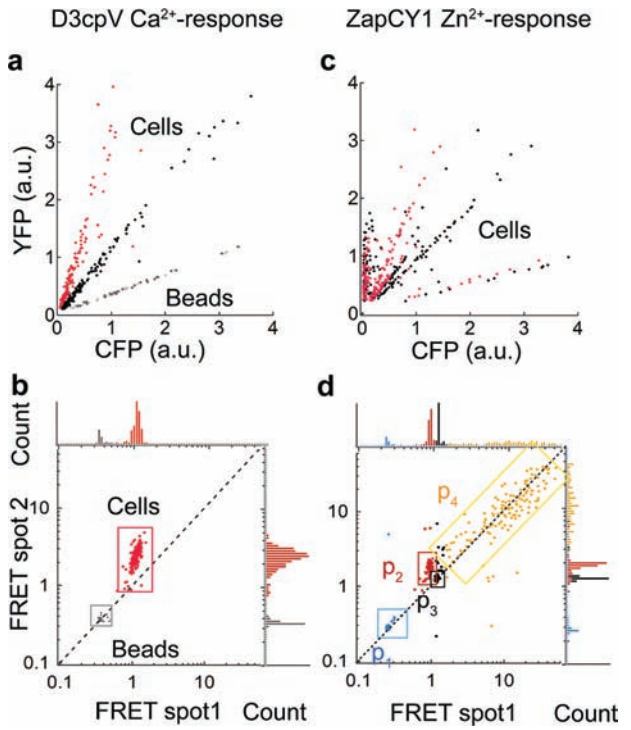

Figure 3. Ca^{2+} and Zn^{2+} sensor responses in microfluidics. (a) Ca^{2+} response of HeLa cells expressing the Ca^{2+} sensor D3cpV at T = 1.29 ± 0.06 s, triggered by a Ca^{2+}-loaded buffer containing 30 mM Ca^{2+} and 49 μM ionomycin: black ●, spot 1; red ●, spot 2. (b) FRET cluster maps (FRET at spot 2 vs FRET at spot 1) for D3cpV-HeLa cells and beads. (c) Zn^{2+} response of HeLa cells expressing the Zn^{2+} sensor ZapCY1 at T = 3.43 ± 0.14 s, triggered by a Zn^{2+}-loaded buffer containing 4 mM Zn^{2+} and 70 μM pyrithione: black ●, spot 1; red ●, spot 2. (d) The FRET cluster map resolves four subpopulations (p1−p4).

The throughput of the single-cell-based FRET change measurement is dictated by the efficiency of the pair-matching technique and n_{crowd} and is variable from 15 cells/s for short time windows (<0.5 s) to ∼1 cell/s for time windows longer than 5 s. Statistical information, such as the average value, standard deviation, and skewness (asymmetry of the probability distribution), of the FRET response for thousands of cells can be obtained within minutes. In comparison with the coefficient of variation (CV) of the doped beads (CV_{beads} = 0.07 ± 0.02), the CV of the cells is larger (CV_{cells} > 0.1), indicating that there is inherent diversity in the sensor expression and FRET ratio in live cells. It has previously been observed that genetically encoded sensors incorporated into living cells demonstrate cell-by-cell variability.[18] The heterogeneity also depends upon the metal-binding state of the sensors. As shown in Figure 3b and observed as a general trend, the FRET at spot 2 (Ca^{2+}- or Zn^{2+}-bound and high FRET ratio) shows a larger CV than that at spot 1 (Ca^{2+}- or Zn^{2+}-free and low FRET ratio). This observation suggests that the FRET efficiency in the metal-bound "active" state is probably more sensitive to small cell-to-cell variations in the sensor molecules (e.g., conformational heterogeneity, post-translational modifications, thermodynamic noise, etc.) or cellular properties (e.g., cell size, stage, metal buffering capacity, etc.).

The two genetically encoded sensors investigated here exhibit distinctly different heterogeneity profiles. In contrast to the roughly unimodal distribution of D3cpV FRET, the ZapCY1 FRET measurement resolved four subpopulations (p_1−p_4) with differences in either the static FRET value or dynamic FRET response (Figure 3c,d). Statistical analysis of the Zn^{2+} response of 3358 cells from various measurements consistently showed that subpopulation p_2 (35.2% ± 3.1%) demonstrates the expected Zn^{2+}-induced response, while the other three (p_1, 4.8% ± 1.5%; p_3, 20.2% ± 2.6%; p_4, 39.8% ± 2.2%) show negligible or weak Zn^{2+} response (Figure 3d). Within distinct subpopulations there is also variability in distribution. The three "unresponsive" subpopulations show low, high, and medium baseline FRET values, suggesting that some of this heterogeneity may arise from proteolysis or sensor instability in the cellular milieu. For example, p_4 exhibits low CFP fluorescence leading to high FRET ratios, and p_1 has low YFP fluorescence leading to low FRET ratios. Importantly, this heterogeneity had not been identified in single-cell microscopy experiments, likely because of the comparatively low throughput of microscopy and the subjective nature of selecting "responsive cells"; to acquire a data set equivalent to that presented in Figure 3d would take at least 35 h on a standard fluorescence microscope, assuming a generous estimate of 10 transfected cells in a field of view and ∼1 h per calibration experiment.

The population-based measurements clearly show that the distribution functions describing the FRET response may take diverse forms, either as a unimodal FRET distribution or as a multimodal distribution with distinct subpopulations. Furthermore, different FRET variability is associated with each sensor state (baseline and active) and with each subpopulation (p1−p4). Our data reveal that two FRET sensors with similar molecular designs give rise to significantly different heterogeneity profiles. The ability to identify and define this heterogeneity has important consequences for sensor design and use.

Recent developments in biosensor design have led to significant improvements in the sensitivity of FRET-based sensors,[17,19,20] but the characterization and optimization of their in vivo kinetic properties has lagged. Well-characterized, fast sensor response kinetics are critical for cellular dynamics studies such as measurements of neural activity.[21,22] The optimal sensor should faithfully report the kinetics of the biological signal; a slow-responding sensor could distort or even miss a transient signal. Capitalizing on the benefits of microfluidics flow control and time-resolved FRET measurements, we expanded this microfluidics method to investigate the kinetics of sensors within the cellular environment. The kinetics were measured as the average FRET of the normal metal-ion-responding population and plotted as a function of cell travel time. The time-resolved response of genetically encoded Ca^{2+} and Zn^{2+} sensors in HeLa cells (Figure 4 and Figure S6) ranged from ∼20 ms (extracellularly displayed sensor) to several seconds (intracellularly expressed sensor).

dx.doi.org/10.1021/ja2101592 | J. Am. Chem.Soc. 2012, 134, 2488−2491

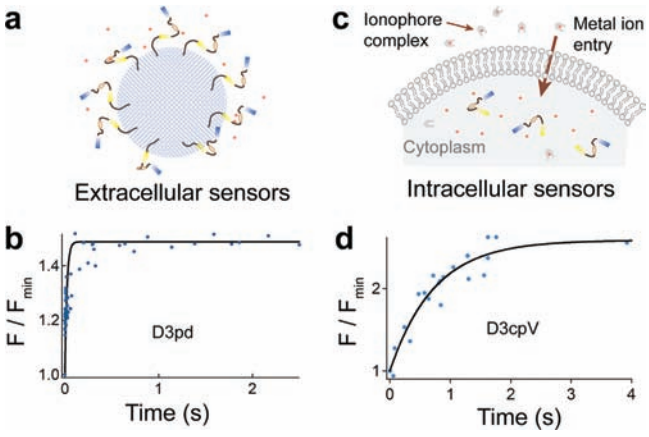

Figure 4. Time-resolved kinetics of sensors in HeLa cells. (a) Extracellular sensor (D3pd) activation. (b) D3pd shows an observed rate constant of k_{obs} = 43 ± 6 s^{-1} upon exposure to 30 mM Ca^{2+}. (c) Intracellular sensor (D3cpv) activation. (d) D3cpV shows an observed response rate constant of k_{obs} = 1.4 ± 0.2 s^{-1} upon exposure to 30 mM Ca^{2+} and 49 μM ionomycin. In (b) and (d), blue ● symbols represent experimental data, and the solid lines were obtained by exponential curve fitting.

Sensors expressed in different cellular locations are likely to exhibit different reaction kinetics. For extracellular-membrane-displayed sensors (Figure 4a), the measured rate constant is largely determined by the intrinsic on/off rates of the sensors and the applied metal-ion concentration. For intracellularly expressed sensors (Figure 4c), the observed kinetics are further limited by the metal-ion transport across the plasma membrane. To examine this effect, we expressed sensors at different cellular locations and compared their response rates under identical experimental conditions. The observed rate constant for D3pd (a surface-displayed Ca^{2+} sensor) was k_{obs} = 43 ± 6 s^{-1} (Figure 4b). In contrast, D3cpV, an intracellular Ca^{2+} sensor with a similar structure, showed ~30-fold slower response kinetics (k_{obs} = 1.4 ± 0.2 s^{-1}) (Figure 4d). The different time scales indicate that metal-ion transport across the cell membrane is likely the rate-limiting step for activation of the intracellular sensor.

Altogether, we have presented a new approach for time-resolved single-cell FRET measurements that is flexible and high-throughput. This method represents a time-resolved generalization of flow cytometry by adding the time dimension to single-cell FRET measurements. This system is capable of controlling and perturbing the extracellular environment and optically probing the kinetics of cellular reactions. We have resolved significantly different heterogeneity profiles associated with different genetically encoded sensors and reported sensor kinetics in different cellular locations, revealing both the inherent kinetics of the sensors and the kinetics of ion transport across the membrane. These measurements would not have been possible using traditional fluorescence microscopy, flow cytometry, or stopped-flow spectroscopy. Our method can be readily extended to large-scale kinetics-based screening or measurement of other optically labeled molecular interactions or reactions in live cells.

■ ASSOCIATED CONTENT

Ⓢ Supporting Information

Supporting figures and materials and methods. This material is available free of charge via the Internet at http://pubs.acs.org.

■ AUTHOR INFORMATION

Corresponding Author

rjimenez@jilau1.colorado.edu; amy.palmer@colorado.edu

Present Address

[§]Department of Bioengineering, University of Colorado Denver, Anschutz Medical Campus, Aurora, CO 80045.

■ ACKNOWLEDGMENTS

We acknowledge financial support from a CU-NIST seed grant, from NIH Grants GM083849 (to A.E.P. and R.J.) and GM084027 (to A.E.P.), and from the JILA Physics Frontier Center (to R.J.). R.J. is a staff member in the Quantum Physics Division of NIST. P.J.D. was supported by a Biophysics Training Grant (T32 GM-065103).

■ REFERENCES

(1) Giepmans, B. N. G.; Adams, S. R.; Ellisman, M. H.; Tsien, R. Y. *Science* **2006**, *312*, 217.

(2) Palmer, A. E.; Qin, Y.; Park, J. G.; McCombs, J. E. *Trends Biotechnol.* **2011**, *29*, 144.

(3) Newman, R. H.; Fosbrink, M. D.; Zhang, J. *Chem. Rev.* **2011**, *111*, 3614.

(4) Lidstrom, M. E.; Konopka, M. C. *Nat. Chem. Biol.* **2010**, *6*, 705.

(5) Bonner, W. A.; Hulett, H. R.; Sweet, R. G.; Herzenberg, L. A. *Rev. Sci. Instrum.* **1972**, *43*, 404.

(6) Taniguchi, Y.; Choi, P. J.; Li, G. W.; Chen, H. Y.; Babu, M.; Hearn, J.; Emili, A.; Xie, X. S. *Science* **2010**, *329*, 533.

(7) Chance, B. *Rev. Sci. Instrum.* **1951**, *22*, 619.

(8) Wilkinson, J. C.; Beechem, J. M.; Staros, J. V. *J. Recept. Signal Transduction Res.* **2002**, *22*, 357.

(9) Whitesides, G. M. *Nature* **2006**, *442*, 368.

(10) Squires, T. M.; Quake, S. R. *Rev. Mod. Phys.* **2005**, *77*, 977.

(11) Beebe, D. J.; Mensing, G. A.; Walker, G. M. *Annu. Rev. Biomed. Eng.* **2002**, *4*, 261.

(12) Constantinescu, V. N. *Laminar Viscous Flow*; Springer: New York, 1995.

(13) Knight, J. B.; Vishwanath, A.; Brody, J. P.; Austin, R. H. *Phys. Rev. Lett.* **1998**, *80*, 3863.

(14) McCammon, J. A.; Harvey, S. C. *Dynamics of Proteins and Nucleic Acids*: Cambridge University Press: Cambridge,U.K., 1987.

(15) Ryan, T. A.; Smith, S. J.; Reuter, H. *Proc. Natl. Acad. Sci. U.S.A.* **1996**, *93*, 5567.

(16) Palmer, A. E.; Giacomello, M.; Kortemme, T.; Hires, S. A.; Lev-Ram, V.; Baker, D.; Tsien, R. Y. *Chem. Biol.* **2006**, *13*, 521.

(17) Qin, Y.; Dittmer, P. J.; Park, J. G.; Jansen, K. B.; Palmer, A. E. *Proc. Natl. Acad. Sci. U.S.A.* **2011**, *108*, 7351.

(18) Dittmer, P. J.; Miranda, J. G.; Gorski, J. A.; Palmer, A. E. *J. Biol. Chem.* **2009**, *284*, 16289.

(19) Horikawa, K.; Yamada, Y.; Matsuda, T.; Kobayashi, K.; Hashimoto, M.; Matsu-ura, T.; Miyawaki, A.; Michikawa, T.; Mikoshiba, K.; Nagai, T. *Nat. Methods* **2010**, *7*, 729.

(20) Mank, M.; Reiff, D. F.; Heim, N.; Friedrich, M. W.; Borst, A.; Griesbeck, O. *Biophys. J.* **2006**, *90*, 1790.

(21) Wallace, D. J.; Borgloh, S.; Astori, S.; Yang, Y.; Bausen, M.; Kugler, S.; Palmer, A. E.; Tsien, R. Y.; Sprengel, R.; Kerr, J. N. D.; Denk, W.; Hasan, M. T. *Nat. Methods* **2008**, *5*, 797.

(22) Tian, L.; Hires, S. A.; Mao, T.; Huber, D.; Chiappe, M. E.; Chalasani, S. H.; Petreanu, L.; Akerboom, J.; McKinney, S. A.; Schreiter, E. R.; Bargmann, C. I.; Jayaraman, V.; Svoboda, K.; Looger, L. L. *Nat. Methods* **2009**, *6*, 875.